Kinetics and Mechanism for the Reaction of Phenyl Radical with Formaldehyde

Y. M. Choi, W. S. Xia,† J. Park, and M. C. Lin*

Department of Chemistry, Emory University, Atlanta, Georgia 30322

Received: February 29, 2000; In Final Form: May 15, 2000

The kinetics and mechanism for the $C_6H_5 + CH_2O$ reaction were investigated by the cavity ringdown spectrometric (CRDS) and pulsed laser photolysis/mass spectrometric (PLP/MS) methods at temperatures between 298 and 1083 K. With the CRDS method, the rate constant was measured by monitoring the decay times of injected probing photons in the absence (t_c^0) and presence (t_c) of the C_6H_5 radical. In the PLP/MS experiment at higher temperatures, the rate constant was determined by kinetic modeling of the absolute yields of C_6H_6. The values of the rate constants obtained by the two different methods agree closely, suggesting that the $C_6H_5 + CH_2O \rightarrow C_6H_6 + CHO$ reaction 1 is the dominant channel. A weighted least-squares analysis of the two sets of data gave $k_1 = (8.55 \pm 0.25) \times 10^4\ T^{2.19\pm0.25} \exp[-(19 \pm 13)/T]$ cm^3 mol^{-1} s^{-1} for the temperature range studied. The mechanism for the $C_6H_5 + CH_2O$ reaction was also elucidated with a quantum-chemical calculation employing a hybrid density functional theory (B3LYP) using the aug-cc-PVTZ basis set. The theory predicts the barriers for the abstraction producing C_6H_6 and the addition giving $C_6H_5CH_2O$ and $C_6H_5OCH_2$ to be 0.8, 1.4, and 9.1 kcal/mol, respectively. The rate constant calculated for the H-abstraction process using the canonical variational transition-state theory with a 1.1 kcal/mol barrier agrees closely with the experimental result over the entire range of temperatures studied.

Introduction

Formaldehyde is a key combustion intermediate in hydrocarbon combustion, its oxidation leads to the formation of CO_2 with the release of a large amount of chemical energy. CH_2O and phenyl radicals coexist in the combustion of benzene;[1] they may coexist in the incipient stage of soot formation. The effects of their interaction in these systems cannot be ascertained if the kinetics and mechanism of the $C_6H_5 + CH_2O$ reaction are not fully characterized.

The first report of the absolute rate constant for the $C_6H_5 + CH_2O$ reaction at room temperature was made by Yu and Lin using the cavity ringdown spectrometric (CRDS) technique in 1993.[2] To our knowledge, there has been no report of its rate constant since.

The reaction may, in principle, take place by the following three product channels:

$$C_6H_5 + CH_2O \rightarrow C_6H_6 + CHO \quad (1)$$

$$\rightarrow C_6H_5CH_2O \quad (2)$$

$$\rightarrow C_6H_5OCH_2 \quad (3)$$

The relative importance of these product channels is not known. To fully elucidate the mechanism for the reaction, we attempted to measure both the total rate constant by the CRDS method[2−7] and the absolute yields of C_6H_6 using the pulsed laser photolysis/mass spectrometric (PLP/MS) technique.[8−12] In addition, we have carried out a quantum chemical calculation to provide the transition state structures and approximate energetics of various species to assist our interpretation of the measured kinetic data. These results are summarized and reported for the first time in this paper.

* Corresponding author. E-mail: chemmcl@emory.edu. Phone: 404-727-2825. Fax: 404-727-6586.

† Permanent address: State Key Laboratory for Physical Chemistry of Solid Surfaces, Institute of Physical Chemistry and Department of Chemistry, Xiamen University, Xiamen, 361005, People's Republic of China.

Experimental Procedure

The rate constant measurement for the $C_6H_5 + CH_2O$ reaction was performed by the CRDS and PLP/MS methods in the temperature range of 298−1083 K. In both cases the CH_2O reactant was obtained by thermal dissociation of known amounts of 1,3,5-trioxane ($c-C_3H_6O_3$) at 850 K.[13] The experimental procedures for the kinetic applications of both CRDS[2−7] and PLP/MS[8−12] methods developed specifically for C_6H_5 reactions have been described in detail before. Hence, only a brief summary of each method is presented below.

CRDS. In this technique, two pulsed lasers were employed for the pump and probe processes. A Lambda Physik LPX 105E excimer laser was used to photodissociate C_6H_5NO (nitrosobenzene) at 248 nm to generate C_6H_5 radicals.[5] A tunable, pulsed dye laser pumped by XeCl excimer laser (Lambda Physik FL 3002) was employed for probing the C_6H_5 radial directly at 504.8 nm where a distinct absorption peak is known to exist.[2,6] Nitrosobenzene was placed on a sealed, fritted glass disk and carried into the reactor via a mixing tube with Ar as a carrier gas.

The CRDS method measures the decay times of injected probing photons in the absence (t_c^0) and presence (t_c) of absorbing species. After multiple internal reflections (typically

10.1021/jp000780y CCC: $19.00
Published on Web 07/11/2000

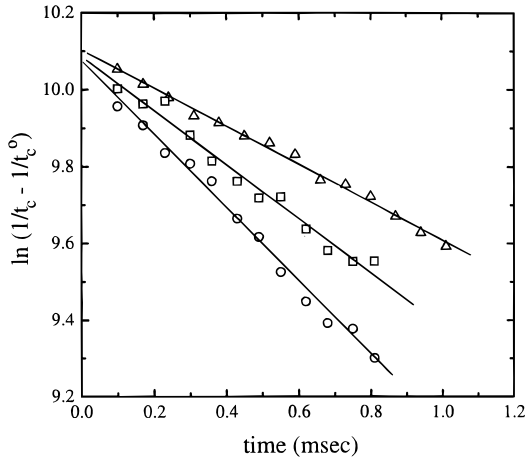

Figure 1. Typical pseudo-first-order decay plots for the $C_6H_5 + CH_2O$ reaction with different, excess reactant concentrations in units of mol/cm^3 at 324 K. (Δ) $[CH_2O] = 0$; (□) $[CH_2O] = 8.62 \times 10^{-9}$; (○) $[CH_2O] = 1.88 \times 10^{-8}$.

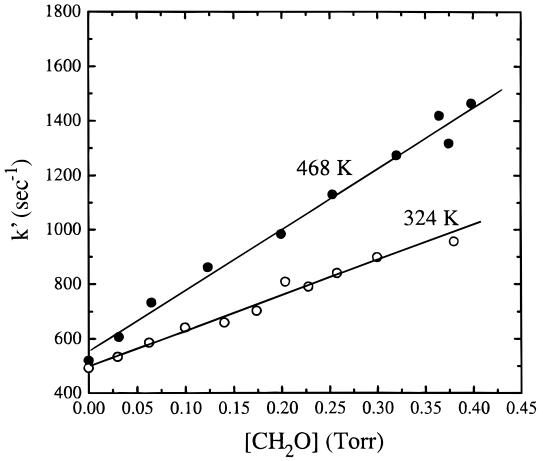

Figure 2. k' vs $[CH_2O]$ at different temperatures. Linear least-squares fit yields the second-order rate constant k'' from their slopes.

$2-3 \times 10^4$ times) inside the high quality resonant cavity employed ($R = 0.99995$), the injected dye laser pulse was typically lengthened from 10 ns to about 20 μs in the absence of an absorbing species. Since the measured values of t_c and t_c^0 are much smaller than the chemical decay time of the radical t, which depends on the concentration of the molecular reactant, the following kinetic relationship holds:[2-7]

$$1/t_c = 1/t_c^0 + (cl\epsilon/nL)[A]_t \qquad \text{(I)}$$

or

$$\ln(1/t_c - 1/t_c^0) = B - k't \qquad \text{(II)}$$

where c is the velocity of light, l is the length of the absorbing medium, ϵ is the extinction coefficient, n is the refractive index of the medium, L is the length of the cavity, $[A]_t = [A]_0 e^{-k't}$ is the concentration of the absorbing species at time t and $B = \ln(cl\epsilon/nL)[A]_0$. According to eq II, the slope of a $\ln(1/t_c - 1/t_c^0)$ vs t plot gives the pseudo-first-order rate coefficient k' for the decay of A, or the C_6H_5 radical, in the presence of a specified molecular reactant concentration, $[CH_2O]$. A standard plot of k' vs $[CH_2O]$ provides the second-order rate constant k'' according to the relationship:

$$k' = k_0 + k''[CH_2O] \qquad \text{(III)}$$

TABLE 1: Experimental Conditions and Measured Rate Constants by the CRDS Method for the Reaction of $C_6H_5 + CH_2O$ at the Temperatures Studied

temp (K)	$[CH_2O]_0$ (Torr)	k_1 (10^{10}cm^3 mol^{-1} s^{-1})[a]
298	0−0.18	2.28 ± 0.26
300	0−0.19	1.98 ± 0.39
313	0−0.38	2.34 ± 0.30
324	0−0.40	2.59 ± 0.10
343	0−0.25	2.85 ± 0.20
346	0−0.18	2.73 ± 0.20
368	0−0.21	3.82 ± 0.54
398	0−0.21	4.09 ± 0.23
418	0−0.21	3.91 ± 0.17
423	0−0.37	4.48 ± 0.47
468	0−0.40	6.55 ± 0.17

[a] The uncertainty represents 1σ.

where k_0 is the first-order decay coefficient of the radical; in the absence of the molecular reactant, it is a convoluted decay rate, consisting of the losses by diffusion, pumping, and recombination reactions.

PLP/MS. The pulsed photolysis of $C_6H_5COCH_3$ at 193 nm (Lamda Physik, Compex 205) was employed as the C_6H_5 radical source in this experiment. The photolytic conversion of acetophenone was in the range of 20−45% depending on photolysis laser energy and $C_6H_5COCH_3$ concentrations. The initial amount of C_6H_5 formed by the photodissociation of $C_6H_5COCH_3$ was determined using NO as the C_6H_5 radical scavenger. The details on the photofragmentation of $C_6H_5COCH_3$ can be found in our previous works.[9-12]

The reactants and the products of the photoinitiated reaction were supersonically sampled from the Saalfeld type quartz reactor,[14,15] ionized by electron impact ionization (35 eV) and detected with a quadrupole mass spectrometer (ABB Extrel C50). The absolute yields of C_6H_6 and $C_6H_5CH_3$ measured in the PLP/MS experiment were determined by careful calibrations, using standard mixtures of known concentrations within the range of product yields, sampled at the same total pressure employed in each run. Kinetic modeling of the absolute concentrations of these products using the mechanism to be presented later gave the rate constants for the formation of C_6H_6 by the $C_6H_5 + CH_2O \rightarrow C_6H_6 + CHO$ direct abstraction reaction. As demonstrated in our previous works,[9,11,12] the quantitative modeling of the absolute yield of $C_6H_5CH_3$ allows us to quantify initial CH_3 and C_6H_5 concentrations under each experimental condition employed.

C_6H_5NO (Aldrich, 97%) was recrystallized using ethanol as solvent and vacuum-dried. Trioxane (Aldrich, 98%), precursor of CH_2O, was purified by standard vacuum distillation. Ar (Specialty Gases, 99.995% UHP grade) used to carry the vapor of nitrosobenzene into the CRD system and He (Specialty Gases, 99.995% UHP grade) used to carry the vapor of acetophenone into the Saalfeld type reactor were employed without further purification.

Computational Methods

The mechanism for the $C_6H_5 + CH_2O$ reaction was elucidated with a quantum-chemical calculation employing a hybrid density functional theory B3LYP, based on Becke's 3-grid integration and exchange functional[16] and the correlation functional of Lee, Yang, and Parr,[17] with Dunning's correlation consistent cc-PVDZ and aug-cc-PVTZ basis sets.[18]

The geometries of the reactants, transition states and products were optimized at B3LYP/cc-PVDZ and their energies calculated at B3LYP/aug-cc-PVTZ level of theory using the structures

TABLE 2: Reactions and Rate Constants[a] Used in the Modeling of the $C_6H_5 + CH_2O$ Reaction in the PLP/MS Experiment.

	reactions	A	n	E_a	ref
1	$C_6H_5 + CH_2O \rightarrow C_6H_6 + CHO$	8.55×10^4	2.19	38	this work
2a	$C_6H_5 + CH_2O \rightarrow C_6H_5CHO + H$	2.91×10^4	2.09	−411	this work[b]
2b	$C_6H_5 + CH_2O \rightarrow C_6H_5CH_2O$	3.79×10^{58}	−15.95	12813	this work[b]
3	$C_6H_5 + CH_2O \rightarrow C_6H_5OCH_2$	3.51×10^2	3.15	8254	this work[b]
4	$C_6H_5CH_2O \rightarrow C_6H_5CHO + H$	1.57×10^{13}	−0.51	3894	this work[b]
5	$C_6H_5 + C_6H_5CHO \rightarrow C_6H_6 + C_6H_5CO$	8.55×10^4	2.19	38	*c*
6	$C_6H_5 + CHO = C_6H_6 + CO$	9.00×10^{13}	0	0	*d*
7	$CH_2O + H \rightarrow CHO + H_2$	2.29×10^{10}	1.05	3280	*e*
8	$C_6H_5CHO + H \rightarrow C_6H_5CO + H_2$	2.29×10^{10}	1.05	3280	*f*
9	$C_6H_5CHO + CH_3 \rightarrow C_6H_5CO + CH_4$	8.93×10^{-13}	7.4	960	*g*
10	$CH_2O + CH_3 = CHO + CH_4$	8.93×10^{-13}	7.4	960	*e*
11	$CH_3 + CHO = CH_4 + CO$	1.21×10^{14}	0	0	*e*
12	$CH_3 + CHO = CH_3CHO$	1.81×10^{13}	0	0	*e*
13	$CH_2O + M = CHO + H + M$	1.20×10^{41}	−6.9	96560	*e*
14	$CH_2O + M = CO + H_2 + M$	2.10×10^{15}	0.0	35010	*e*
15	$CHO + M = H + CO + M$ / H_2/2.00/ H_2O/6.00/ CH_4/2.00/ CO/1.50/ CO_2/2.00/ CH_2O/3.00/ HE/ 0.70/	1.87×10^{17}	1.0	7000	*e*
16	$C_6H_5 + CH_3 = C_6H_5CH_3$	1.38×10^{13}	0	46	11
17	$C_6H_5 + C_6H_5 = C_{12}H_{10}$	1.39×10^{13}	0	111	8

[a] Rate constants are defined by $k = AT^n\exp(-E_a/RT)$ and in units of $cm^3\ mol^{-1}s^{-1}$, E_a is in the units of cal/mol, the rest of the mechanism can be found in ref 11. [b] RRKM calculations at $P = 3$ Torr. [c] Assumed based on the reaction rate of $C_6H_5 + CH_2O \rightarrow C_6H_6 + CHO$. [d] Assumed to be the same as $CH_3 + CHO$. [e] Reference 26. [f] Assumed to be the same as $CH_2O + H$. [g] Assumed to be the same as $CH_2O + CH_3$.

TABLE 3: Experimental Conditions,[a] Product Yields,[b] and Modeled Rate Constants[c] for C_6H_6 Formation in the PLP/MS Experiment at the Temperatures Studied

					$[C_6H_6]_t$		$[C_6H_5CH_3]_t$	
temp (K)	$[C_6H_5COCH_3]_0$	$[C_6H_5]_0$[d]	$[CH_2O]_0$	k_1[e]	exptl	modeled	exptl	predicted[f]
476	4.87	2.60	117.07	0.67	0.60	0.60	0.73	0.71
566	4.79	2.68	117.07	0.89	0.66	0.66	0.70	0.76
641	4.82	2.61	117.15	1.21	0.72	0.72	0.74	0.72
668	5.41	2.14	117.57	1.32	0.67	0.68	0.52	0.54
767	5.56	1.98	117.57	1.72	0.70	0.70	0.49	0.45
833	4.85	2.70	117.65	2.09	0.89	0.89	0.67	0.65
903	4.56	2.99	117.65	2.37	0.97	0.97	0.73	0.70
1083	6.08	1.47	117.57	3.40	0.65	0.65	0.21	0.18

[a] All concentrations are given in milliTorr; total pressure 3 Torr with He as a carrier gas. [b] Product yields were measured at $t = 15$ ms at their plateaus. Typically 2 or 3 runs were carried out for each temperature. [c] In units of $10^{11}\ cm^3\ mol^{-1}\ s^{-1}$. [d] Determined by NO titration measuring C_6H_5NO yields. [e] Obtained by fitting the observed C_6H_6 yields. [f] Predicted absolute yields using k_{16} reported in ref 11.

predicted by the former, smaller basis set calculations. The predicted vibrational frequencies and geometries of the species relevant to the interpretation of the measured kinetic data are summarized in Appendix A and Appendix B, respectively.

The rate constants for the three product branching reactions were calculated with the predicted geometries and energies using the transition-state theory (TST) for reaction 1 and the Rice−Ramsperger−Kassel−Marcus (RRKM) theory for reactions 2 and 3. These results will be compared with experimentally determined values later.

Results and Discussion

Experimental Kinetic Data. As mentioned in the preceding section, two complementary techniques were employed to measure the rate constant for the $C_6H_5 + CH_2O$ reaction in the temperature range of 298−1083 K.

With the CRDS technique, the rate constants were measured in the temperature range between 298 and 468 K at 40 Torr pressure using C_6H_5NO as the C_6H_5 radical source with Ar as the carrier gas. Figure 1 presents typical pseudo-first-order plots for the decay of C_6H_5 at 324 K in the presence of the different amounts of CH_2O at 40 Torr total pressure. The slope of the plot, the pseudo-first-order rate coefficient (k') of the reaction at each CH_2O concentration, was obtained by a standard weighted least-squares analysis. The values of k' varying with the concentration of CH_2O are shown in Figure 2; the slopes of k' vs $[CH_2O]$ plots directly give the second-order rate constants k''. The experimental conditions and measured rate constants at each temperature studied are summarized in Table 1.

In the PLP/MS experiment at higher temperatures as described above, $C_6H_5COCH_3$ was employed as the C_6H_5 radical source as in our previous studies on $C_6H_5 + H_2$,[9] CH_4[11] and i-C_4H_{10}.[12] Kinetic modeling of the absolute yields of C_6H_6 and $C_6H_5CH_3$, assuming the initial concentrations of C_6H_5 and CH_3 to be the same in the photolysis process,[11] was performed using SENKIN program[19] in conjunction with CHEMKIN thermodynamic library.[20] The reaction mechanism is similar to the previously established one for $C_6H_5 + H_2/CH_4/i$-C_4H_{10} reactions and only additional reactions involving CH_xO ($x = 1,2$), and the two key recombination reactions of C_6H_5 are summarized in Table 2. The results of kinetic modeling for the absolute yields of C_6H_6 and $C_6H_5CH_3$ are summarized in Table 3 together with the detailed experimental conditions employed.

The directly measured values of k'' by CRDS and the kinetically modeled values of k_1 by PLP/MS for the $C_6H_5 + CH_2O$ reaction are graphically presented in Figure 3 together with theoretically predicted result (to be discussed below) for comparison. It is important to note that the values of the rate constants determined by the two different methods agree closely,

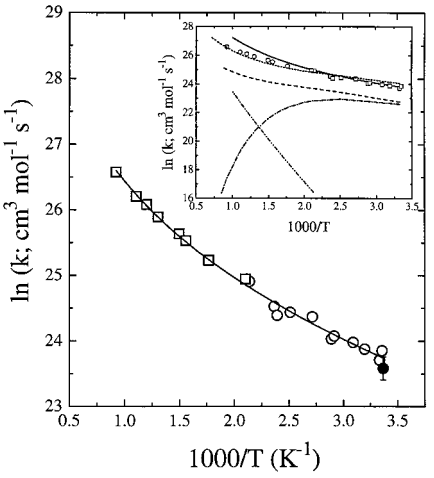

Figure 3. Arrhenius plot of (○) k'' by CRDS and (□) k_1 by PLP/MS. (●) Reference 2. The solid curve is the result of a weighted least-squares analysis. Inset: Comparison of the experimental and theoretically predicted results for the $C_6H_5 + CH_2O$ reaction. Symbols, experimental results (this work); solid (k_1), dashed (k_{2a}), dashed−dotted (k_{2b}), and dashed−double-dotted (k_3) curves are the TST or RRKM results calculated with TS parameters predicted by B3LYP/cc-PVDZ with $E_1^0 = 0.8$, $E_2^0 = 1.4$, and $E_3^0 = 9.1$ kcal/mol, calculated at the B3LYP/aug-cc-PVTZ level of theory. RRKM calculations for k_2 and k_3 were performed at 3 Torr pressure to be consistent with the PLP/MS experiment. Dotted (k_1) curve is the CVTST result calculated with TS parameters predicted by B3LYP/cc-PVDZ with $E_1^0 = 1.1$ kcal/mol giving the best overall fit.

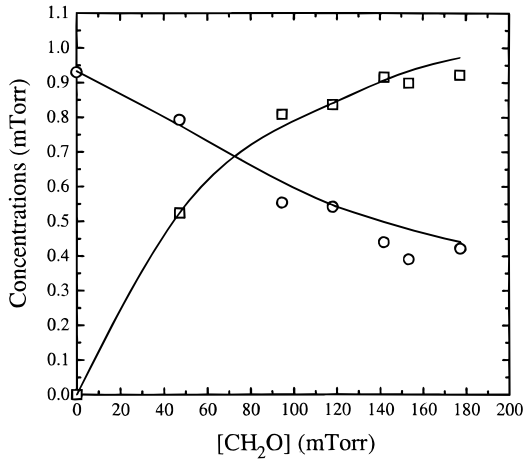

Figure 4. Concentration profiles of (□) C_6H_6 and (○) $C_6H_5CH_3$ as a function of $[CH_2O]$ at the total pressure of 3 Torr. Reaction conditions: $[C_6H_5COCH_3]_0 = 4.69$ and $[C_6H_5]_0 = 2.44$ mTorr. Solid curves are predicted values using the mechanism in Table 3.

suggesting that reaction 1 is the dominant channel. A weighted least-squares analysis of the rate constants obtained from both experiments gave

$$k_1 = k'' = (8.55 \pm 0.25) \times 10^4\, T^{2.19 \pm 0.25} \exp[-(19 \pm 13)/T]\ \mathrm{cm^3\,mol^{-1}\,s^{-1}}$$

for the temperature range of 298−1083 K.

To test the validity of our k_1 given above, we performed an additional set of experiments at 852.5 K by measuring the concentrations of C_6H_6 and $C_6H_5CH_3$ as functions of CH_2O with the total pressure kept constant. As shown in Figure 4, the measured yields of benzene and toluene can be reasonably accounted for with kinetically predicted values.

As aforementioned, the measurement of toluene, which is one of the major products formed in the pulsed laser photolysis of

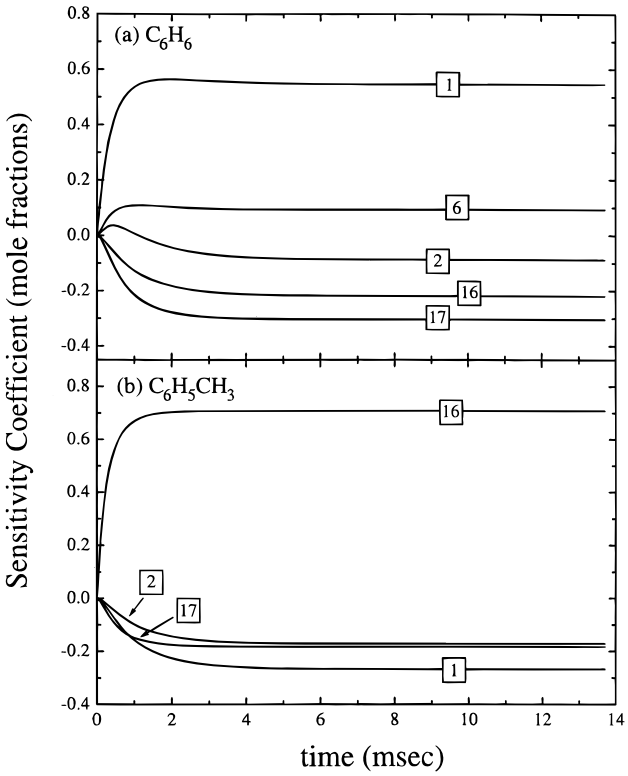

Figure 5. Sensitivity analyses for (a) C_6H_6 and (b) $C_6H_5CH_3$ at 833 K in the PLP/MS experiment. The conditions are given in Table 2. The sensitivity coefficient for the effect of reaction j on the mole fraction of species i X_i is defined as $S_{ij} = \partial X_i/\partial k_j$ (k_j/X_i); where k_j is the rate constant for reaction j.[19]

$C_6H_5COCH_3$, is very important because its formation solely by the recombination of C_6H_5 with CH_3 allows us to reliably monitor the initial concentrations of the C_6H_5 and CH_3 radicals. The result of our sensitivity analysis presented in Figure 5 clearly indicates that the yields of C_6H_6 and $C_6H_5CH_3$ depend overwhelmingly on reactions 1 and 16, respectively. It is worth noting that the yields of toluene can be quantitatively accounted for by the model with our previously reported value for k_{16}.[11]

Reaction Mechanism. As alluded to in the Introduction section, the reaction of C_6H_5 with CH_2O may take place by three distinct channels producing four different sets of products:

$$C_6H_5 + CH_2O \rightarrow C_6H_6 + CHO \quad (1)$$

$$\rightarrow C_6H_5CH_2O^{\dagger} \rightarrow C_6H_5CHO + H \quad (2a)$$

$$\rightarrow C_6H_5CH_2O^{\dagger} \rightarrow C_6H_5CH_2O\ (+M) \quad (2b)$$

$$\rightarrow C_6H_5OCH_2\ (+M) \quad (3)$$

In reaction 2, "†" stands for internal excitation. These product channels have been confirmed by our transition-state search at the B3LYP/cc-PVDZ level of theory. The energy barriers predicted at the B3LYP/aug-cc-PVTZ level for reactions 1−3 are, respectively, 0.8, 1.4, and 9.1 kcal/mol. The potential energy curves for the individual product channels are presented in Figure 6, and the computed rate constants with TST or RRKM theory are shown in the inset of Figure 3 for comparison with experimental data.

As shown in Figure 3, the predicted rate constant for the H-abstraction reaction 1 with a small tunneling correction agrees very closely with the experimental result, particularly at $T <$ 600 K. At higher temperatures, the value predicted by the

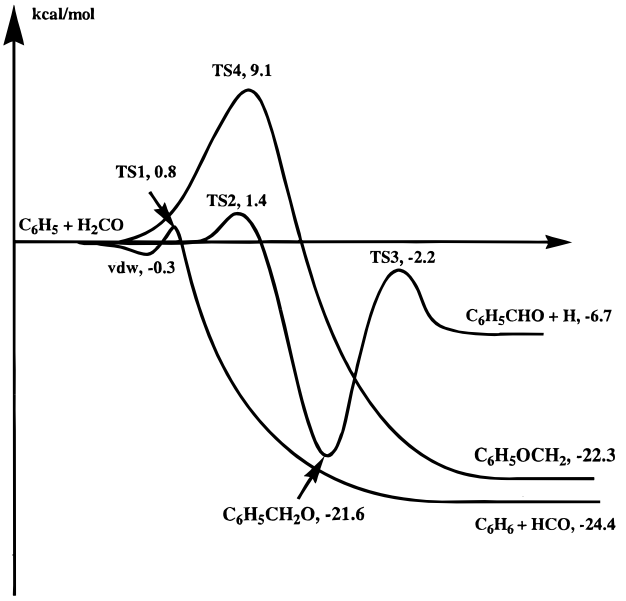

Figure 6. Potential energy curves for reactions 1−3 calculated at the B3LYP/aug-cc-PVTZ//cc-PVDZ level of theory. All energies given include zero-point energy corrections.

conventional TST[21] deviates from experiment noticeably. To account for the deviation, we have performed a canonical variational transition state theory (CVTST) calculation near the col region using the maximum free energy criterion.[22] The result of this calculation, employing the approach described previously for the CHO + O_2 abstraction reaction,[23] led to a much better agreement between theory and experiment over the entire range of temperature employed. The reaction barrier used in the latter calculation was slightly increased from 0.8 to 1.1 kcal/mol (which is well within the accuracy of the DFT technique) to give the best overall match. In these calculations, the torsional vibration (88 cm^{-1}) between the C_6H_5 and HCO groups was taken as a free internal rotation; whereas the two nearly degenerate rocking motions (57 and 58 cm^{-1}) were treated either as vibrations or as a 2-D hindered rotation using the method of Hase and Zhu.[24] Both calculations give essentially indistinguishable results.

Reaction (2a) is expected to give C_6H_5CHO as a minor product under our higher-temperature, low-pressure (3 Torr) PLP/MS conditions. At 3 Torr RRKM calculations predicted $k_{2a} = 2.91 \times 10^4\ T^{2.09}\ \exp(207/T)$ $cm^3\ mol^{-1}\ s^{-1}$ and $k_{2b} = 3.79 \times 10^{58}\ T^{-15.95}\ \exp(-6448/T)$ $cm^3\ mol^{-1}\ s^{-1}$; they were included in our modeling for k_1 (see Table 3). Under the conditions employed, $k_1 \gg (k_{2a} + k_{2b})$. Experimentally, we have carried out a careful search for the formation of C_6H_5CHO to no avail, because of the small predicted concentration and of the overlap in the mass peaks of benzaldehyde and acetophenone.

Reaction (3) is too slow to be competitive with (1) or (2). The $C_6H_5OCH_2$ adduct can, in principle, also produce C_6H_5-CHO by the isomerization/decomposition reaction.[25] A detailed theoretical calculation on this reaction is currently underway.

It should be mentioned that both CH_2O and $C_6H_5COCH_3$ are thermally stable at the highest temperature (1083 K) within the time scale employed (several tens of milliseconds). CH_2O was also found to be stable at 193 nm near 1000 K; no detectable change in the $m/z = 30$ peak was noted when the reaction mixture was photolyzed at 193 nm in the absence of acetophenone.

Conclusion

The kinetics and mechanism for the $C_6H_5 + CH_2O$ reaction have been investigated by the CRDS and PLP/MS methods in the temperature range of 298−1083 K. In both cases, the CH_2O reactant was obtained by thermal dissociation of known amounts of 1,3,5-trioxane (c-$C_3H_6O_3$) at 850 K. By the CRDS technique, the rate constant was measured in the temperature range between 298 and 468 K at 40 Torr pressure, using C_6H_5NO as the C_6H_5 radical source with Ar as a carrier gas. In the PLP/MS experiment at higher temperatures using $C_6H_5COCH_3$ as the C_6H_5 radical source, the rate constants were determined by kinetic modeling of the absolute yields of C_6H_6 and $C_6H_5CH_3$. The result of our sensitivity analysis indicates that the yields of C_6H_6 and $C_6H_5CH_3$ depend overwhelmingly on reactions 1 and 16, respectively. The values of the rate constant determined by the two different methods agree closely, suggesting that reaction 1 is the dominant channel. A weighted least-squares analysis of the rate constants obtained from both experiments gave $k_1 = (8.55 \pm 0.25) \times 10^4\ T^{2.19 \pm 0.25} \exp[-(19 \pm 13)/T]$ $cm^3\ mol^{-1}\ s^{-1}$ for the temperature range of 298−1083 K. The mechanism for the $C_6H_5 + CH_2O$ reaction was also elucidated with a quantum-chemical calculation employing a hybrid density functional theory B3LYP with the cc-PVDZ basis set for geometry optimization and with the aug-cc-PVTZ basis set for energy calculation. The predicted rate constant for the H-abstraction reaction 1 using the canonical variational transition-state theory with a 1.1 kcal/mol barrier agrees closely with the experimental result over the entire range of temperatures studied.

Acknowledgment. The authors are grateful for the support of this work from the Basic Energy Sciences, Department of Energy, under Contract DE-FG02-97-ER14784. We are also thankful to Dr. W. H. Kirchhoff for providing us sufficient NERSC CPU time for the quantum-chemical calculations.

Appendix A: Frequencies and Moments of Inertia for Reactants, Products, TS1, and vdw of the $C_6H_5 + CH_2O = C_6H_6 + CHO$ Reaction Calculated at the B3LYP/cc-PVDZ Level

species	I_i (amu)	υ_j (cm^{-1})
C_6H_5	288.8054, 323.6028, 612.4081	401, 425, 597, 614, 673, 720, 813, 893, 966, 981, 998, 1022, 1048, 1070, 1164, 1164, 1292, 1340, 1457, 1465,1584,1639, 3166, 3173, 3185, 3188, 3199
H_2CO	6.4262, 46.6468, 53.0731	1186, 1253, 1515, 1833, 2868, 2921
HCO	2.6243, 40.5280, 43.1523	1094, 1936, 2605
C_6H_6	318.4651, 318.4651, 636.9301	415, 415, 618, 618, 692, 723, 867, 867, 988, 988,1014,1020, 1023, 1059, 1059, 1162, 1187, 1187, 1358, 1364,1507,1507, 1646, 1646, 3166, 3177, 3177, 3193, 3193, 3204
vdw	358.2534, 2017.1851, 2375.4384	27, 39, 64, 83, 117, 182, 406, 428, 596, 616, 674, 729, 829, 912, 979, 980, 1005, 1022, 1051, 1076, 1164, 1171, 1194, 1256, 1303, 1338, 1457, 1469, 1507, 1582, 1637, 1817,2875, 2947, 3163, 3170, 3181, 3184, 3196
TS1	358.7869, 1764.0174, 2122.8043	*588(i)*, 57, 58, 88, 205, 359, 403, 442, 510, 608, 690, 731, 836, 841, 911, 976, 1006, 1017, 1041, 1076, 1152, 1167, 1174, 1212, 1243, 1306, 1342, 1454, 1482, 1533, 1604,1634, 1847, 2820, 3159, 3163, 3174, 3179, 3194

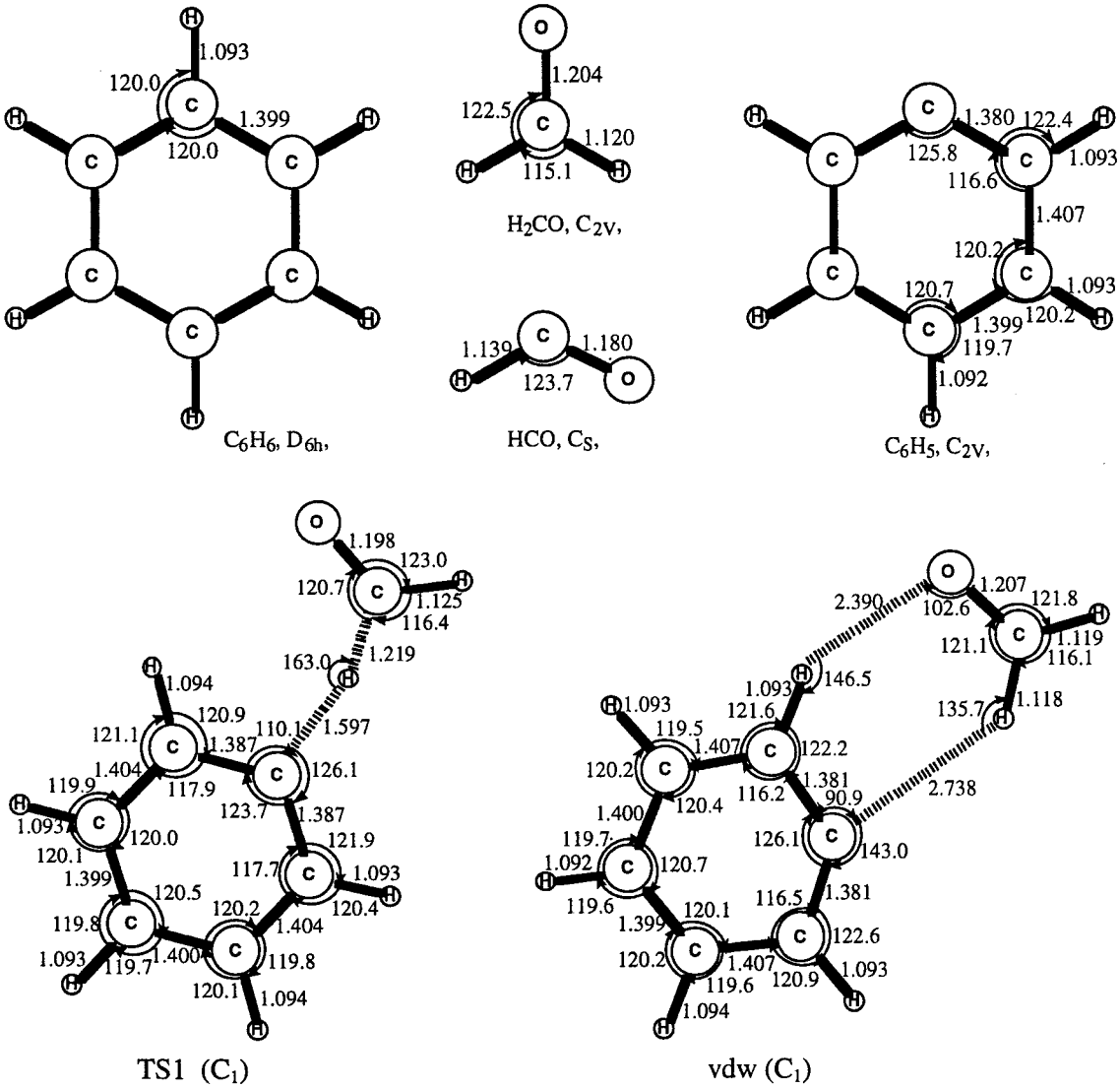

Appendix B. Molecular and transition state geometries for the $C_6H_5 + CH_2O = C_6H_6 + CHO$ reaction optimized at the B3LYP/cc-PVDZ level of theory. Bond lengths are in angstroms and angles in degrees.

References and Notes

(1) Zhang, H.-Y.; McKinnon; J. K. *Combust. Sci. Technol*. **1995**, *107*, 261.

(2) Yu. T.; Lin, M. C. *J. Am. Chem. Soc*. **1993**, *11*, 4371.

(3) Yu, T.; Lin, M. C.; Melius, C. F. *Int. J. Chem. Kinet.* **1994**, *26*, 1095.

(4) Yu, T.; Lin, M. C. *J. Am. Chem. Soc*. **1994**, *116*, 9571.

(5) Yu, T.; Lin, M. C. *J. Phys. Chem*. **1994**, *98*, 2105.

(6) Park, J.; Lin, M. C. *Cavity-Ring-Down Spectrometry-A New Technique for Trace Absorption Measurements*; ACS Publication Series 720, American Chemical Society: Washington, DC, 1999; Chapter 13, p 196.

(7) Park, J.; Chakraborty, D.; Bhusari, D. M.; Lin, M. C. *J. Phys. Chem. A* **1999**, *103*, 4002.

(8) Park, J.; Lin, M. C. *J. Phys. Chem. A* **1997**, *101*, 14.

(9) Park, J.; Dyakov, I. V.; Lin, M. C. *J. Phys. Chem. A* **1997**, *101*, 8839.

(10) Park, J.; Lin, M. C. *Recent Research Development in Physical Chemistry*; Transworld Research Network: India, **1998**; Vol. 2, p 965.

(11) Tokmakov, I. V.; Park, J.; Gheyas, S. I.; Lin, M. C. *J. Phys. Chem. A* **1999**, *103*, 3636.

(12) Park, J.; Gheyas, S. I.; Lin, M. C. *Int. J. Chem. Kinet*. **1999**, *31*, 645.

(13) Aldridge, K. H.; Liu, X.; Lin, M. C.; Melius, C. F. *Int. J. Chem. Kinet.* **1991**, *23*, 947.

(14) Wyatt, J. R.; DeCorpo, J. J.; McDowell, W. V.; Saalfeld, F. E. *Rev. Sci. Instrum*. **1974**, *45*, 916.

(15) Wyatt, J. R.; DeCorpo, J. J.; McDowell, M. V.; Saalfeld, F. E. *Int. J. Mass Spectrum. Ion Phys*. **1975**, *16*, 33.

(16) (a) Becke, A. D. *J. Chem. Phys*. **1993**, *98*, 5648. (b) Becke, A. D. *J. Chem. Phys*. **1992**, *96*, 2155. (c) Becke, A. D. *J. Chem. Phys*. **1992**, *97*, 9173.

(17) Lee, C.; Yang, W.; Parr, R. G. *Phys. Rev. B* **1988**, *37*, 785.

(18) (a) Woon, D. E.; Dunning, T. H., Jr. *J. Chem. Phys*. **1993**, *98*, 1358. (b) Kendall, R. A.; Dunning, T. H., Jr.; Harrison, R. J. *J. Chem. Phys*. **1992**, *96*, 6796.

(19) Lutz, A. E.; Kee, R. J.; Miller, J. A. SENKIN: A FORTRAN Program for Predicting Homogeneous Gas-Phase Chemical Kinetics with Sensitivity Analysis. Sandia National Laboratory Report No. SAND 87-8009; Sandia National Laboratory: Livermore, CA, 1989.

(20) Kee, R. J.; Rupley, F. M.; Miller, J. A. CHEMKIN−II: A FORTRAN Chemical Kinetics Package, for the Analysis of Gas-Phase Chemical Kinetics. Sandia National Laboratory Report No. SAND 89-8009; Sandia National Laboratory: Livermore, CA, 1988.

(21) Laidler, K. J.; King, M. C. *J. Phys. Chem*. **1983,** *87*, 2657.

(22) Truhlar, D. G.; Grev, R. S.; Garrett, B. C. *J. Phys. Chem*. **1983**, *87*, 3415.

(23) Hsu, C.-C.; Mebel, A. M.; Lin, M. C. *J. Chem. Phys*. **1996**, *105*, 2346.

(24) Hase, W. L.; Zhu, L. *Int. J. Chem. Kinet*. **1994**, *26*(*4*), 407.

(25) Mulcahy, M. F. R.; Tucker, B. G.; Williams, D. J.; Wilmshurst, J. R. *Aust. J. Chem*. **1967**, *20*, 1155.

(26) NIST Chemical Kinetics Database. National Institute of Science and Technology: Washington, DC, 1998 (2Q98).